Journal of Materials Chemistry B

ARTICLE ELECTRONICAL SUPPLEMENTARY INFORMATION

A novel hybrid nanofibrous strategy to target progenitor cells for a cost-effective *in situ* angiogenesis

N. Sachot[a,b], O.Castaño[*a,b,c], H. Oliveira[d], J. Martí-Muñoz[a,b], A. Roguska[e], J. Amedee[d], M. Lewandowska[f], J.A. Planell[a,b] and E. Engel[g,a,b].

*Corresponding author: ocastano@ibecbarcelona.eu

ORMOGLASS composition by EDS

%	OG5 10-90	OG5 20-80
Ti	5.5 ± 0.8	5.7 ± 0.9
Ca	45.5 ± 1.6	44.1 ± 1.8
P_2	44.5 ± 0.4	45.2 ± 1.8
Na_2	4.5 ± 1.2	5.1 ± 0.9

Table S1. Composition of the hybrid fibers (molar percentages).

Viscosity optimization

The viscosity values of PLA-ORMOGLASS blends measured after hydrolysis process. After some minutes of stabilization, the viscosity of the blend is maintained over time. Results showed that after addition of the ORMOGLASS, the viscosity of the polymeric solution decreased (**table S2**). The blend containing the higher ORMOGLASS quantity was the less viscous. However, both slurries had the appropriate viscosity to enable the fabrication of fibers by electrospinning.

	Viscosity (mPa·s)	**Temperature (°C)**
PLA	665 ± 13	24.6
OG5 10-90	369 ± 9	25.4
OG5 20-80	284 ± 4	25.1

Table S2. Viscosity of the PLA solution and hybrid blends (4% polymeric solution) after few minutes of homogenization.

Alignment quantification by Fast Fourier Transform (FFT)

FFT allows the characterization of the alignment of the samples by processing the image into mathematically defined ''frequency'' space and then a radial quantification using imageJ image processing software[1] and the plugin developed by William O'Connnell[2].

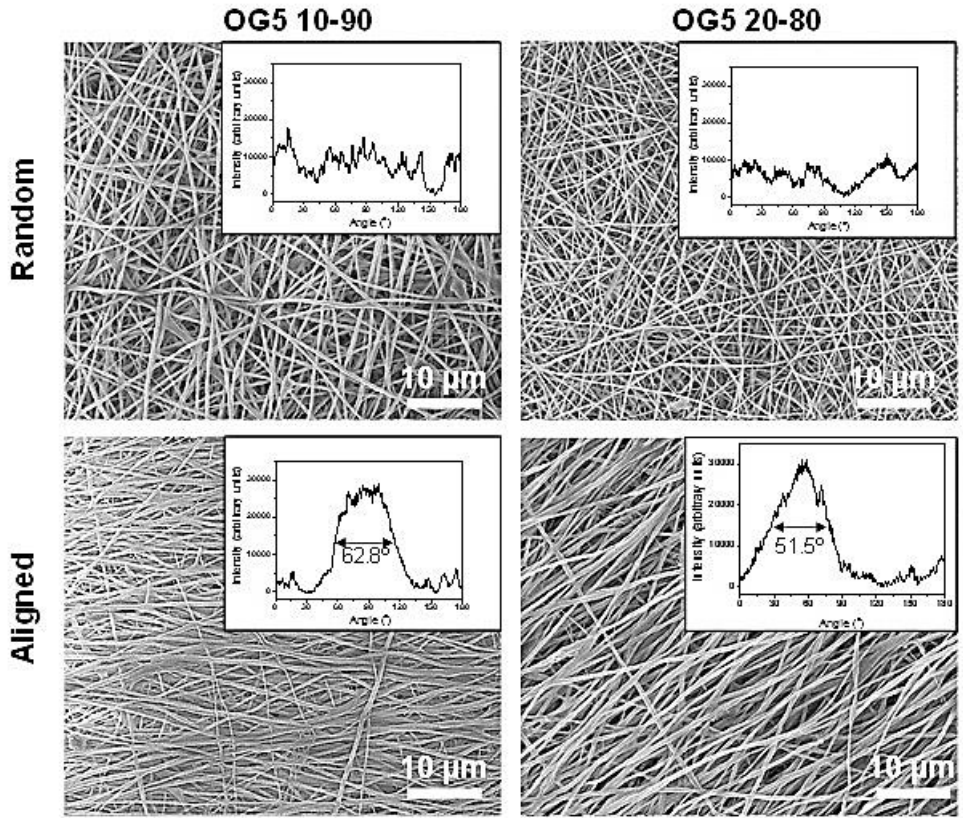

Figure S1. Representative FESEM images of a random d an aligned mats. The pixel intensity plots vs the angle of acquisition has been added in the insets. The FWHM was calculated to assess the level of angle disorientation.

Contact angle measurements

As observed on **figure S2**, the incorporation of the glass gel improved the wettability of the scaffolds. In comparison to the contact angle values of PLA fibers (higher than 100°), hybrid fibers exhibited lower values for both ratios and both fiber distributions. **Figure S3** shows the influence of the fibers organization on the contact angle measurement depending on which direction is the measurement performed.

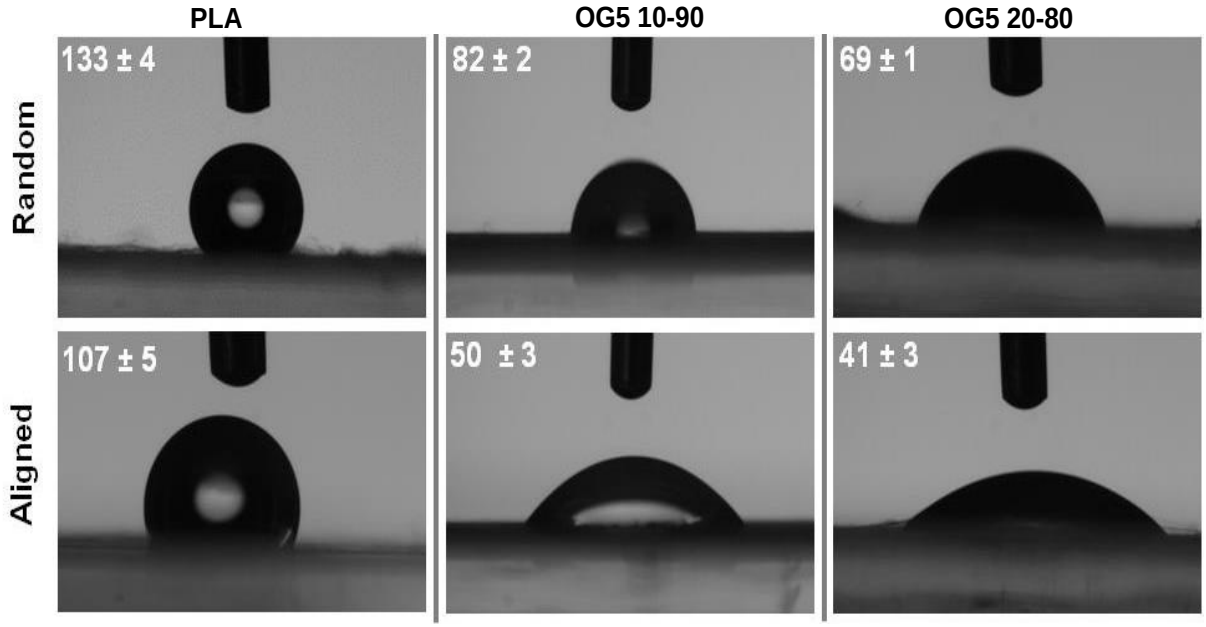

Figure S2. Contact angle pictures and measurements performed on PLA and hybrid fibers.

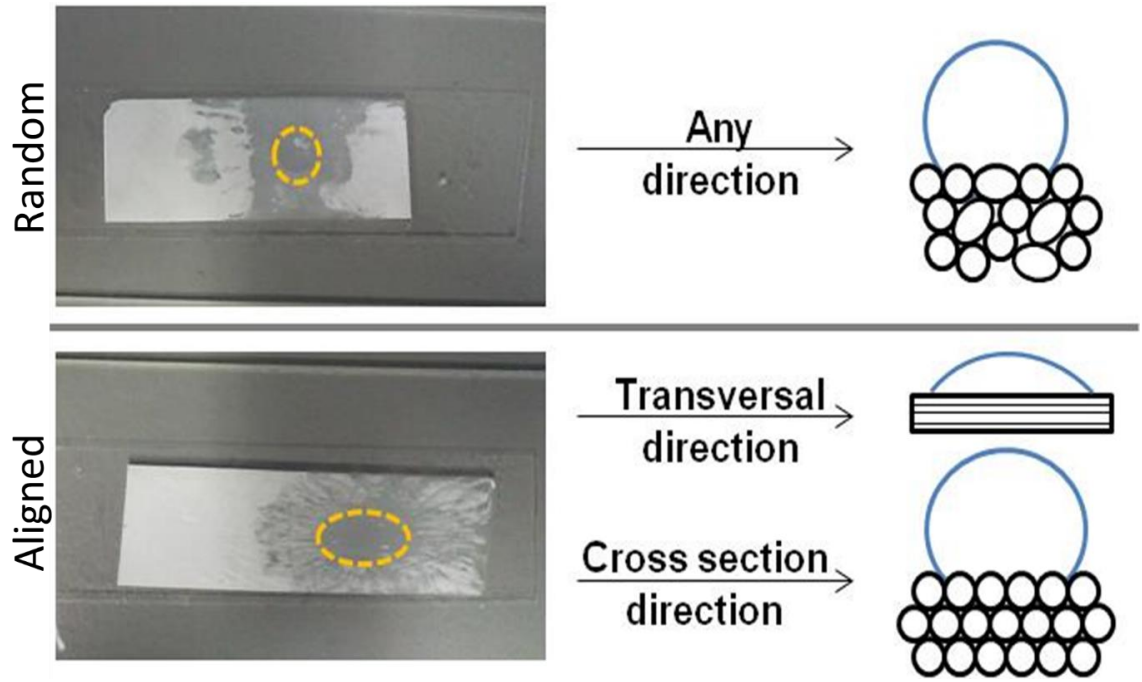

Figure S3. Pictures and schematic representation of the water drop behaviour on random and aligned fibers depending on the positioning of the sample.

Polymer thermal properties

Figure S4 displays the DSC thermograms obtained for PLA and hybrid fibers (first and second heating ramps). Neither the crystallization peak nor the evident melting peak (only a very small bump, not considered as significant enough to conclude anything about melting) were observed on the first heating ramp curve. The sharp peak observed at ~ 122°C on the curve of the OG5 20-80 fibers corresponds to a measurement artefact and was not considered for data interpretation. Results showed that the Tg values were slightly shifted towards lower values when ORMOGLASS was incorporated in the polymeric fibers. The higher the amount of ORMOGLASS in the fibers, the lower the T_g, although these differences were very slight.

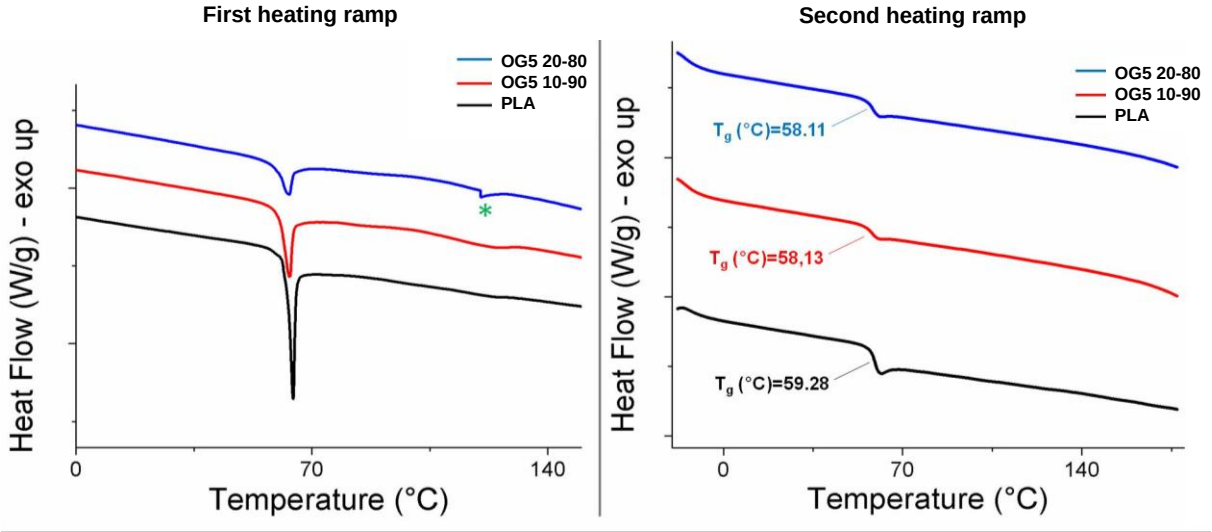

Figure S4. Thermograms of PLA and hybrid fibers obtained by DSC (first and second heating ramps, *: measurement artefact).

Thermogravimetric analysis coupled Fourier Transform Infrared Spectroscopy

FTIR was coupled with TGA analysis in order to determine which compounds were degrading during the TGA assay of OG5 20-80 aligned fibers (see **table 3S**). The spectra related to the decomposition of the compounds are presented in **figure S5**. Based on the literature [3,4], the peaks 1 and 2 observed for the hybrid fibers were both assigned to alkylphosphate molecules. The presence of two peaks associated to the same kind of molecules can be explained by the nature of the species found in the phosphorous precursor (mono and diethyl phosphate)[5]. The third peak is typically due to the decomposition of PLA (lactide and other compounds associated to the degradation of PLA: carbon dioxide, carbon monoxide, acetaldehyde…)[6,7].

	T Peak 1 (°C)	T Peak 2 (°C)	T Peak 3 (°C)	Remaining Weight (%)	Fibers Glass content (%)*
PLA	-	-	360	0	0
OG5 10-90	217	245	355	15.5	25.5
OG5 20-80	223	245	341	24.3	40.8

Table S3. Table summarizing the thermal characteristics of the PLA and hybrid fibers obtained by TGA (*: calculated considering the weight associated to peaks 1 and 2).

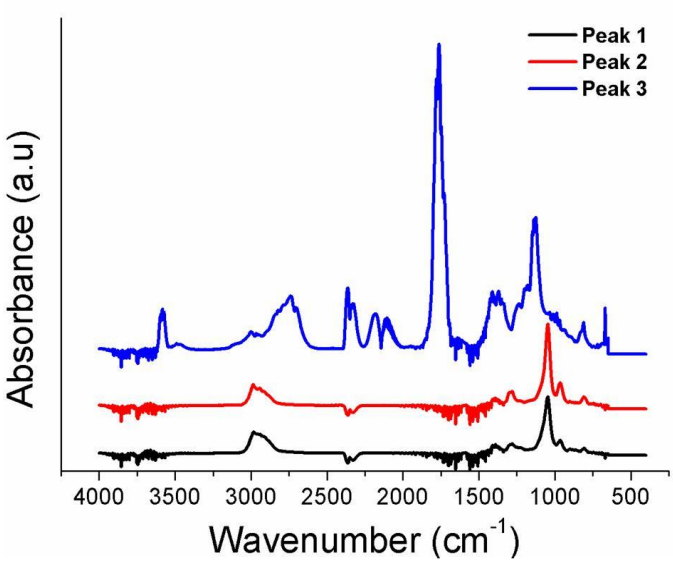

Figure S5. FTIR spectra of compounds vaporizing during the thermal degradation of OG5 20-80 aligned fibers.

Mechanical Properties

The hybrid fibers exhibited the higher mechanical properties. Both approached Young's Modulus and Yield Strength were improved in comparison to PLA fibers. The higher the content of the ORMOGLASS, the higher the approached Young's modulus (**figure S6**). The yield strength appeared not to be affected by the ORMOGLASS content itself. The same values were calculated for both compositions. Moreover, aligned fibers exhibited better mechanical properties than random ones. Aligned fibers had, for example, a Young's modulus that doubled random ones. Samples' aspect after the tensile assay can be found in **figure S7**.

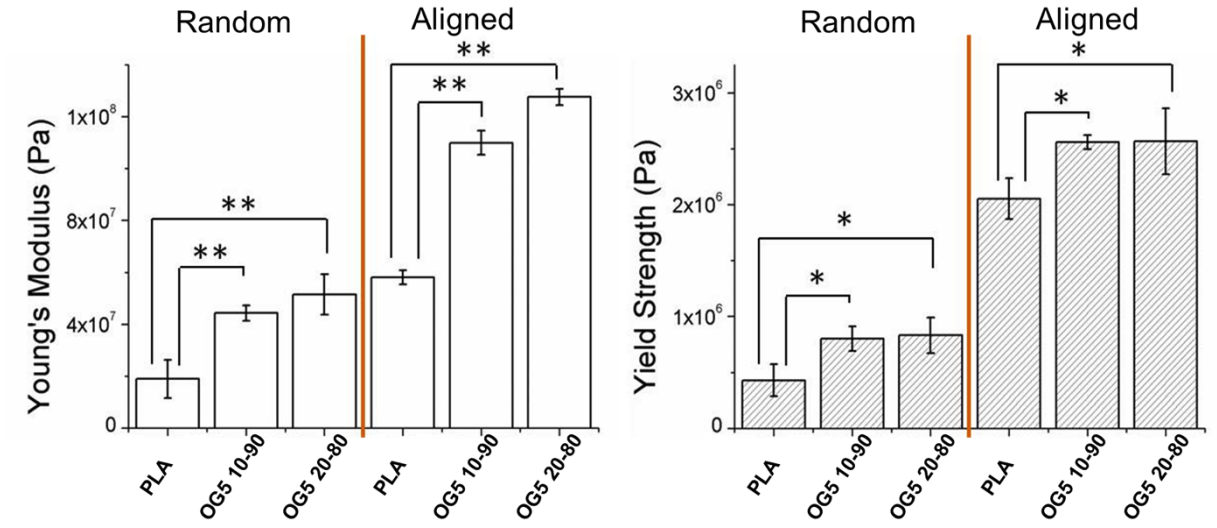

Figure S6. Approached Young's Modulus and Yield Strength of PLA and hybrid fibers (tensile tests - *: statistical difference $p < 0.05$, **: statistical difference $p < 0.001$).

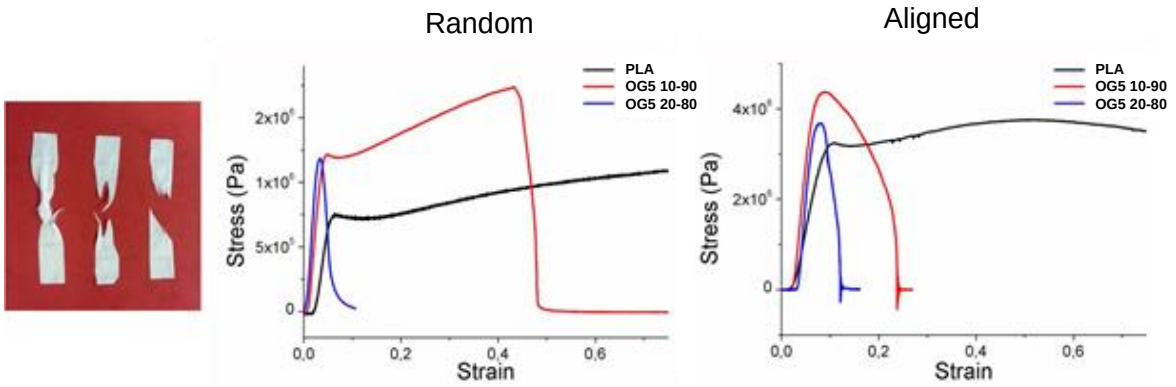

Figure S7. Pictures of random hybrid fibers after tensile tests and typical strain-stress curves obtained for the random and hybrid mats.

Protein adsorption

Qualitative measurements performed with FTIR revealed that BSA adsorbed better on the hybrid fibers than on the PLA ones (**figure S8**). Indeed, after immersion in the protein solution, both hybrids exhibited signals of the amide I and II (chemical groups of the BSA molecule)[8,9], attesting to the presence of BSA on the fibers. To the contrary, these signals were not observed in the polymeric fibers.

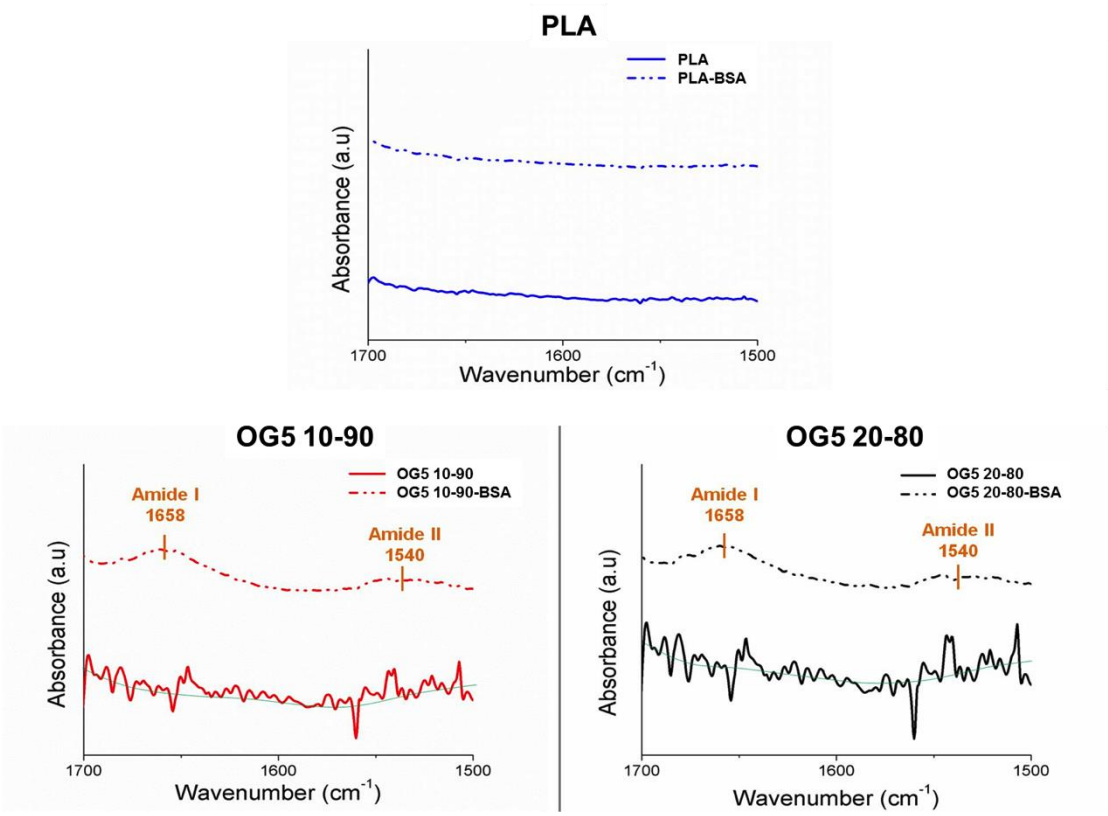

Figure S8. FTIR spectra obtained for PLA and hybrid fibers before and after the protein adsorption test.

pH of the immersed hybrids.

Initially pink, the culture medium turned yellow when OG5 20-80 fibers were immersed (**figure S9**). pH measurements indeed clearly demonstrated that immediately after fiber immersion, the pH of the medium dropped critically. For comparison, the measurements were also performed in SBF, and the pH drop was even higher in this case. However, because SBF and medium are known to act as buffers of the pH, the measurement was additionally performed in water to evaluate the real pH changes in an unbuffered solution. The pH dropped from 7.4 to 2.7 in water. A significant pH decrease would be critical for cells and would lead to cytotoxicity [10]. Therefore, it was necessary to add a buffer in the medium in order to control the pH. Based on the pH curved obtained in medium containing 20 mM of HEPES, it can be seen that the pH remained quasi stable. In fact, according to the pictures, the colour of the medium did not change significantly, suggesting that this HEPES concentration was suitable for cellular assays.

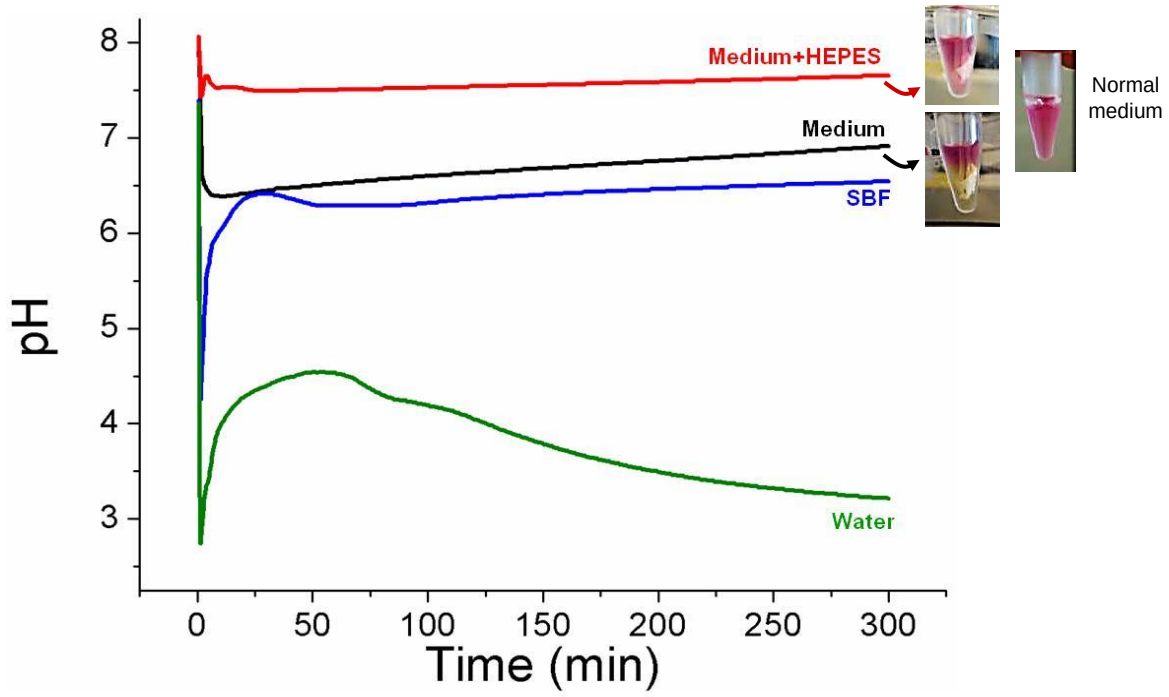

Figure S9. Evolution of pH after OG5 20-80 fiber immersion in different solutions. Pictures show the colour changes observed when fibers were immersed in medium.

pH vs time for protein adsorption

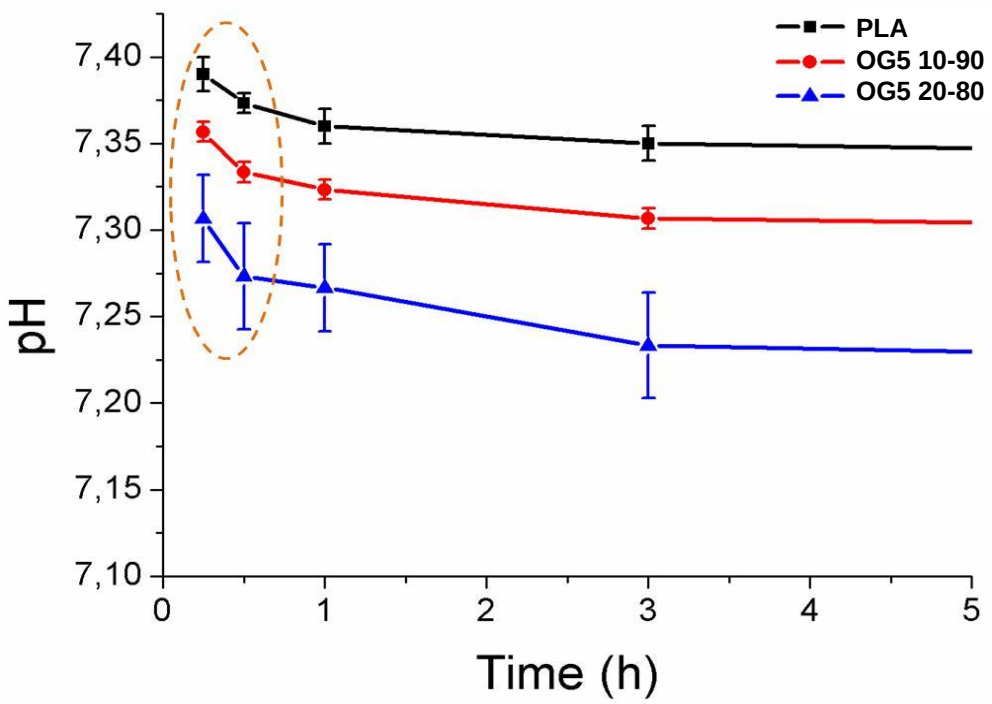

Figure S10. pH measurements of the solution in which the BSA adsorption test was performed (orange circle denotes the range of pH of the solution during the time of the assay: 30min).

Fiber's surface charge

The surface electrostatic potential of the fibers was evaluated by measuring the ZP. **Figure S11** in the supporting information shows the curves obtained. **Table S4** summarizes the isoelectric point values (IEP, pH value at ZP = 0) and ZP values after for pH = 7 (indicative value chosen for comparison). Globally, the produced fibers were less electronegative than the PLA ones. At pH = 7, the IEP values of the hybrids were very close to each other. At this pH however, the fibers with the higher ORMOGLASS content (OG5 20-80 fibers) appeared to be the less electronegative.

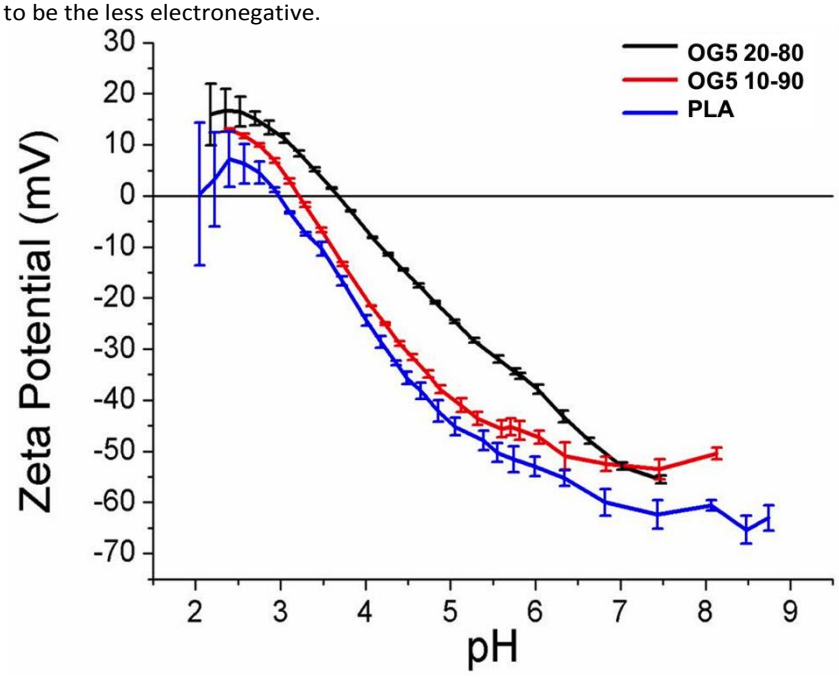

Figure S11. pH dependence of the zeta potential of the PLA and hybrid fibers.

	ZP (mV)	IEP
PLA	-61	3.0
OG5 10-90	-52	3.2
OG5 20-80	-51	3.7

Table S4. Electrostatic potential (ZP) at pH = 7.4 and isoelectric point (IEP) values of the fibers surface.

In vivo assays.

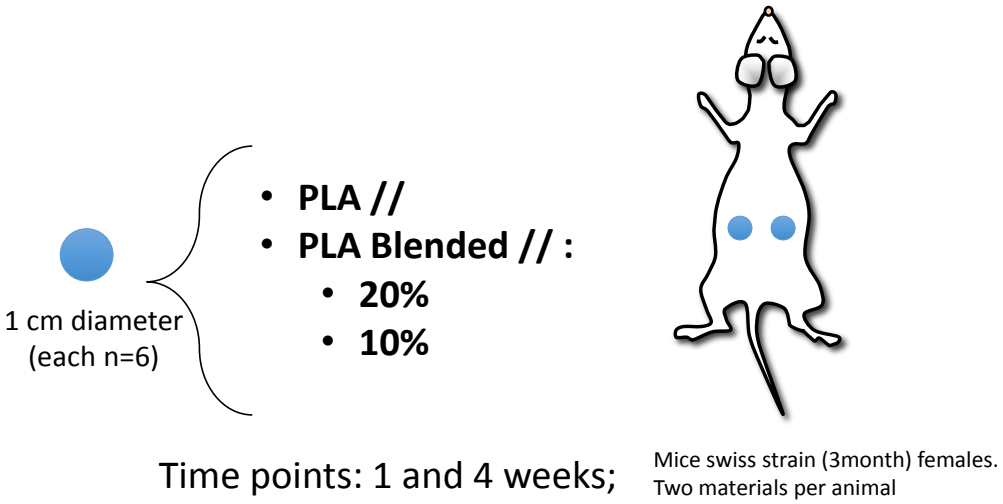

Figure S12. Graphical description of the samples implanted in the dorsus of the mice.

References:

1 W. S. Rasband, *US Natl. Inst. Heal. Bethesda, USA, http//imagej.nih.gov/ij/*, 1997, 2014.

2 C. Ayres, G. L. Bowlin, S. C. Henderson, L. Taylor, J. Shultz, J. Alexander, T. A. Telemeco and D. G. Simpson, *Biomaterials*, 2006, **27**, 5524–5534.

3 L. George, K. Sankaran, K. S. Viswanathan and C. K. Mathews, *Appl. Spectrosc.*, 1994, **48**, 7–12.

4 R. L. Bagalawis, J. Carlson and J. Walsh, *Qualitative method for the detection of triethylphosphate in aqueous solutions*, 2003.

5 D. Carta, D. M. Pickup, R. J. Newport, J. C. Knowles, M. E. Smith and K. O. Drake, *Phys. Chem. Glas.*, 2005, **46**, 365–71.

6 C. Vogel and H. W. Siesler, *Macromol. Symp.*, 2008, **265**, 183–194.

7 F. Kopinke, M. Remmler, K. Mackenzie, M. Möder and O. Wachsen, *Polym. Degrad. Stab.*, 1996, **53**, 329–342.

8 O. Mahony, O. Tsigkou, C. Ionescu, C. Minelli, L. Ling, R. Hanly, M. E. Smith, M. M. Stevens and J. R. Jones, *Adv. Funct. Mater.*, 2010, **20**, 3835–3845.

9 J. Kim, J. Cho, P. M. Seidler, N. E. Kurland and V. K. Yadavalli, *Langmuir*, 2010, **26**, 2599–608.

10 M. Uo, M. Mizuno, Y. Kuboki, A. Makishima and F. Watari, *Biomaterials*, 1998, **19**, 2277–84.